

A robust approach to the design of an electromagnetic shield based on pyrolytic carbon

Patrizia Lamberti,^{1,a} Polina Kuzhir,^{2,3,b} and Vincenzo Tucci^{1,c}

¹*Dept. of Information and Electrical Engineering and Applied Mathematics, University of Salerno, 84084 Fisciano (SA), Italy*

²*Research Institute for Nuclear Problems of Belarusian State University, 220030 Minsk, Belarus*

³*Tomsk State University, 634050 Tomsk, Russia*

(Received 13 May 2016; accepted 27 June 2016; published online 6 July 2016)

A robust approach to the design of an electromagnetic shield based on ultra-thin pyrolytic carbon (PyC, 5÷110 nm) films is proposed. Finite Element Method (FEM) simulations and Monte Carlo based tolerance analysis are used to show that even a deviation of 15÷20% from the nominal values of the most important design parameters of the PyC film, i.e. its thickness and sheet resistance, does not significantly affect the wanted level of electromagnetic interference shielding efficiency (EMI SE). The ranges of the SE show that EMI shield based on PyC film is characterized by a robust behavior with respect to the variation of such parameters due to the production processes. Therefore, since the PyC can be produced on a scalable basis, is chemically inert, significantly transparent in the visible range and can be deposited onto both metal and dielectric substrates, including flexible polymers, it may be appropriate for the highly demanding technological needs associated to the graphene revolution and can be developed from laboratory to mass production applications. © 2016 Author(s). All article content, except where otherwise noted, is licensed under a Creative Commons Attribution (CC BY) license (<http://creativecommons.org/licenses/by/4.0/>). [<http://dx.doi.org/10.1063/1.4958298>]

I. INTRODUCTION

As the microwave spectrum becomes more and more crowded and electromagnetic compatibility problems become more stressful, one needs new functional materials with high electromagnetic (EM) interference shielding efficiency (EMI SE) for EM coatings, shields and filters working in the microwave frequency bands.

Carbon is an attractive material for electromagnetic shielding because of its low density and high electrical conductivity of the carbon allotropes with dominated sp^2 bonds.¹ There are graphite, carbon blacks, multi-walled and one third of single-walled carbon nanotubes, onion-like carbons, pyrolytic carbon, carbon porous monoliths, graphite nanoplatelets and graphene.^{2–18} These forms of carbon are used as fillers in dielectric polymers to transform them into shielding materials providing EMI SE ability at the level of 5–20 dB per 1–4 mm coating depending on the level of its ac and dc conductivity that preserve flexibility, chemical inertness, ease of shaping and lightness of the polymer matrix.^{12–18} In some cases it is also necessary to add third fraction, i.e. clay, as a fluffier agent (see Ref. 16–18). Another interesting option is to use flexibility, small sheet resistance, optical and IR transparency, ultra small thickness and ultra light-weight of carbonaceous and graphene films.^{8–11} Among them CVD made Pyrolytic Carbon (PyC) films¹⁹ are of special interest. By combining high optical transparency²⁰ and small sheet electrical resistance, flexibility

^aCorresponding author plamberti@unisa.it

^bpolina.kuzhir@gmail.com

^cvtucci@unisa.it

and robustness,²¹ these films have a strong application potential. In particular, PyC films can be deposited onto both dielectric and metal substrates of any shape and size, while in EM applications, they can compete with graphene heterostructures¹¹ or single-walled carbon nanotubes films.²²

The EMI SE of the film is determined by absorption of the EM energy inside the film and the reflection from its surface, whereas the multiple internal reflections do not play role as the phase shift is very small in the thickness of the thin film. When EM coating thickness is larger than its skin depth, a conducting layer reflects almost 100% of the incident radiation. The high reflectance is undesirable since the reflected radiations become new source of EM pollution,²³ the shielding material should be able to absorb a considerable part of the incident radiation. It could be achieved for conducting thin films much thinner than their skin depth in case their thickness correspond to a sheet conductance close to the admittance of free space, 2.7 mS. Such an admittance matching condition²⁴ can be met for 75 nm thick PyC film.⁹

In order to succeed with producing effective device providing effective EMI shielding on a scalable basis which can be retranslated to commercial applications clear instructions have to be given on how significantly the most important parameters can deviate from the “nominal” values determined from the theory. These deviations could cause errors for the realization of the device and its performance could be very different from what was expected. In some cases, the designed device, such as the shield, could not even be physically realizable or “reliable”.^{25–28}

In this paper, we propose a robust approach to the design of an electromagnetic shield based on PyC film (see Fig. 1) toward developing scalable protocol for possible commercial applications.

The design that satisfies the customer constraints also in presence of given tolerances on the physical or geometrical parameters is called Robust Design.²⁵

In the framework of this approach, we assume that parameters of the device are characterized by some uncertainty (uncontrollable physical parameters) or variability given by technological processes (controllable physical parameters).^{27–30} The robust design allows us to create a device that meets the specifications ensuring the required robustness by minimizing the Performance Function (PF, i.e. the EMI SE in this case) of the system.^{26,27}

The EMI SE of the PyC film is obtained numerically by solving the electromagnetic problem with a commercial FEM-based code developed in Comsol Multiphysics®. The good agreement of the numerically computed SE with that obtained analytically for this simple geometry and configuration opens a wide range of applications to the model. In fact it can be adopted even in different configurations which are not resolvable in closed form (complex 2D or 3D geometry, not classical electrical behavior of the material and/or evaluation of the effect of different physics like the mechanical one).

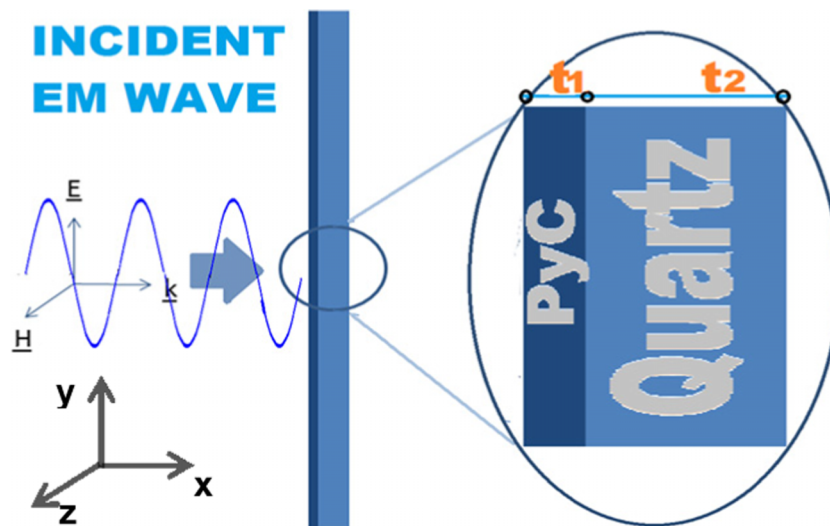


FIG. 1. Two dimensional sketch of the considered double-layer EM shield.

II. MATERIAL AND METHODS

A. The FEM model

In order to numerically analyze and design the shield, a model is developed by using a commercial software (Comsol Multiphysics®, RF module) implementing the Finite Element (FE) technique.

In Fig. 2 the shield origin is in $x=0$. Perfect Matched Layers (PMLs) are introduced in order to model the infinitely long free space around the shield. PML acts as an adapted load in such a way that impacting electromagnetic waves are not reflected causing errors in the simulation.

By considering the plane wave applied to the “Port 1”, the EMI SE can be obtained from the following equation:

$$SE (dB) = -S_{21} = -20 \log \left| \frac{E_t}{E_i} \right| = 20 \log \left| \frac{E_i}{E_t} \right| \quad (1)$$

where E_t and E_i are the amplitudes of the transmitted and incident waves, respectively. Fig. 3 shows the calculated amplitude of the transmitted wave obtained with parameters listed in Table I for a PyC film thickness of $t_1=110\text{nm}$. In particular the data reported in Fig. 3 are obtained by performing 100 simulations with frequency settled at equidistant value in the range [20–40] GHz. One can observe from Fig. 3(a) that the amplitude and phase of the wave change due to the PyC film at $x=0$. The reliability of the numerical solution is tested by comparing the simulated data with the analytical solution.³¹

B. Robust design problem

We studied the EMI SE at central frequency of the Ka band, i.e. at $f = 30\text{GHz}$. The thickness t (controllable factor) and electrical conductivity σ (not controllable) of the PyC film are considered as design uncertain variables. The choice of the thickness variability δt is determined by the accuracy of the deposition process and the inevitable film non-uniformity (i.e. 0.3nm). The conductivity variability is set at 10% around the nominal value:

$$\sigma = \sigma_0 \pm \delta\sigma_0 = (5 \pm 0.5) \times 10^4 \text{S/m} \quad (2)$$

$$t_0 \in [9 \div 110] \text{ nm} \quad t = t_{oi} \mp \delta t_0 \quad (3)$$

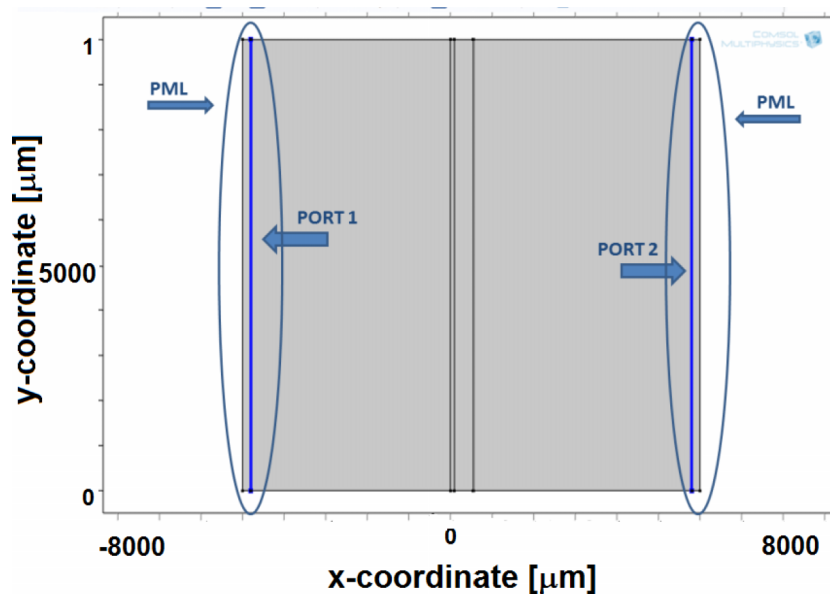


FIG. 2. Adopted 2-dimensional z -section of the infinitely long (i.e. in y direction) double layer EM shield in Fig. 1 for the FEM simulation of a plane wave incident along x axis.

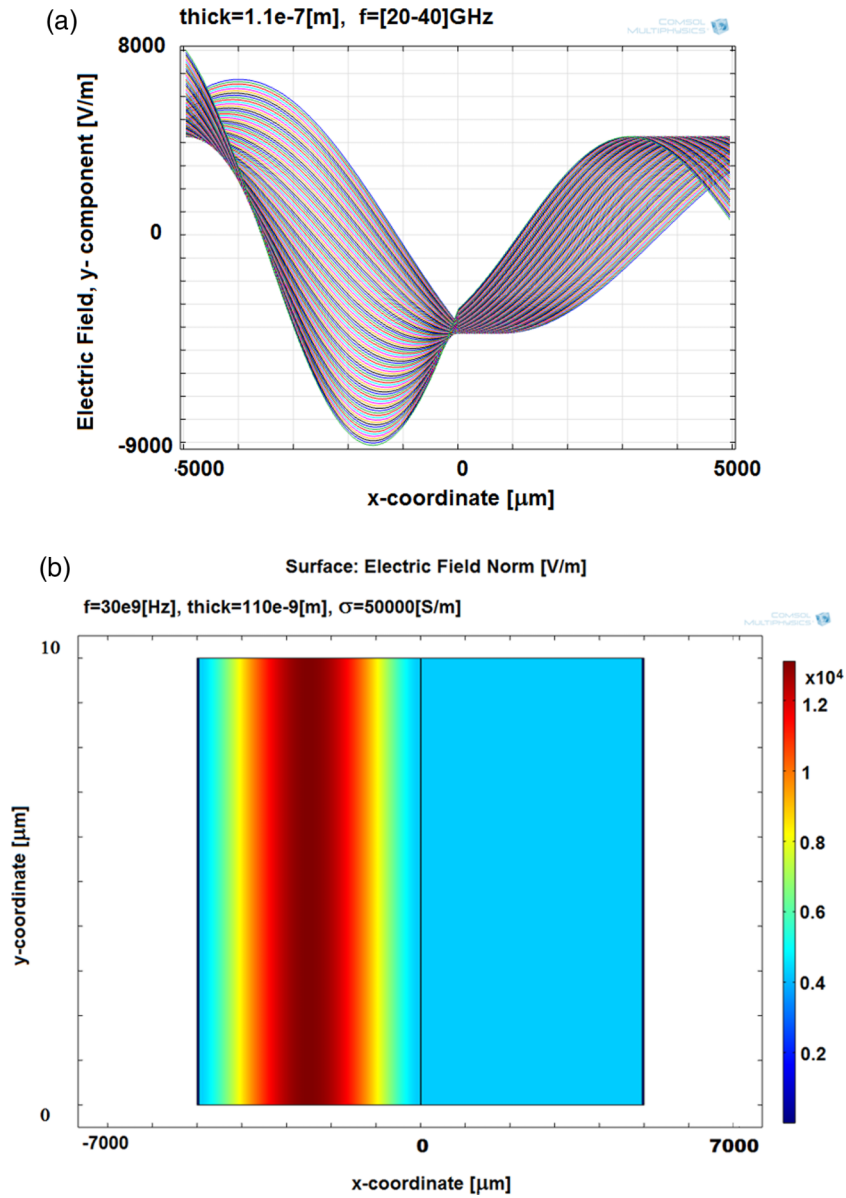


FIG. 3. y-component of the electric field for a PyC-SiO₂ shield with thickness $t_1=110\text{nm}$ and $t_2=500\mu\text{m}$: a) parametric simulation of the spatial variation in the $(x-y)$ plane with respect to the frequency in the Ka-band; b) color map of the norm for the central frequency $f=30\text{GHz}$.

Monte Carlo (MC) analysis is often used for searching the optimal design parameters set especially if the PF is, as in this paper, numerically computed. In this case, the search space is explored by means of randomly chosen trials leading to scattered data for the PF. The result is the best nominal solution of the problem, but not all the work done to evaluate the performance function is used. Actually it is possible to exploit the samples located in each neighborhood of a solution in order to obtain information about the sensitivity of the PF by looking at the maximum and minimum values that it achieves. Nevertheless the MC approach leads to an underestimate sensitivity and therefore it requires a high number of trials in order to obtain a “robust” result. Instead the Vertex Analysis (VA) method is able to provide a reliable estimation of the function extremes especially in the case of monotonic behavior. Such a result, which can be demonstrated by recurring to the Weierstrass theorem,³² is not valid anymore in presence of not-simply connected domains.²⁶

TABLE I. Adopted Material and Geometrical Characteristics for PyC and SiO₂ domains.

Domain	PyC	SiO ₂
electrical conductivity σ [S/m]	5×10^4	0
Relative permittivity ϵ_r	1	4.2
Layer Thickness [m]	$9 \times 10^{-9} \div 110 \times 10^{-9}$	5×10^{-4}
Complex Amplitude of the Wave Vector K [m ⁻¹]	$7695 - j7695$	1288
Characteristic Impedance ζ [Ω]	$1.54 + j1.54$	183
Penetration Depth δ [m]	1.3×10^{-5}	infinite

To overcome such problems a searching algorithm based on a combination of Monte Carlo (MC) and VA approaches is here implemented in Matlab® code in order to find the robust solution with a low number of function calls.

A 2-dimensional parameter space is considered like that reported in Fig. 4(a). Each point (t_0, σ_0) in this space leads to a particular shield design. The SE at the given frequency of 30GHz is numerically computed by exploiting the FEM model presented before. The solution space $SE(t_0, \sigma_0)$ is reported in Fig. 4(b).

The robust solution is obtained by minimizing the following index:

$$S_{box} = \frac{W_{SE(t, \sigma)}}{\langle SE(t_i, \sigma_i) \rangle_{(t_i, \sigma_i) \in box}} = \frac{\max_{(t_i, \sigma_i) \in box} SE(t_i, \sigma_i) - \min_{(t_i, \sigma_i) \in box} SE(t_i, \sigma_i)}{\frac{1}{N} \sum_{i=1}^N SE(t_i, \sigma_i)} \quad (4)$$

where $W_{SE(t, \sigma)}$ is an estimation of the range amplitude for the numerically computed PF in correspondence of the nominal solution (t, σ) due to the assumed variation of the design parameters, whereas $\langle SE(t_i, \sigma_i) \rangle_{(t_i, \sigma_i) \in box}$ is the mean value assumed by the PF in each box sampled with N points. When the parameters span the sample-box, the lower S_{box} the more robust is the nominal solution. Here N is different for each nominal solution and it is obtained by considering a neighborhood of almost three points over the vertices of the box.

III. RESULTS

The parameters space is sampled initially by considering 2000 MC trials obtained by assuming uniformly distributed and uncorrelated uncertainty parameters in the range defined with (2) and (3). According to the adopted procedure that guarantees at least three points in each boxes in addition to the vertices around the nominal solution, a total of 2130 simulations has to be considered leading to obtain the scattered data plot shown in Fig. 5. The most robust nominal solution $(t, \sigma)_{RD} = (110\text{nm}, 5 \times 10^4 \text{S/m})$ is obtained by minimizing (4), i.e. $S_{box} = 0.15$ (see Fig. 6), with the PF spanning the range $[5.7, 6.5] \text{ dB} = 6.1 \text{ dB} \pm 7\%$, that is obtained from the scattered data of Fig. 5.

It means that, by considering this nominal solution, the SE will be affected at minimum by the parameter variations, especially with respect to the uncontrollable factor σ_0 . The range of $W_{SE(t, \sigma)}$ will be less than 15% of the mean value as indicated in Fig. 6 by the value of 0.15 reached by S_{box} . It is interesting to compare this robust solution with the experimental data achieved with similar parameter values. In particular, in Ref. 9 the case of a structure with PyC thickness of 110nm, deposited on a silica substrate of 530nm is considered. The measured SE value for this sample is 7.49dB at 30GHz with the incident field on the opposite side with respect to the case considered here. Nevertheless, by considering the basic measurement error of the EM attenuation over the range 0 to 25 dB,⁸ that is $\delta|S_{21}| = \pm(0.6 + 0.06|S_{21}|) = \pm 1.05$, leads to a SE in the range $[6.44, 8.54] \text{ dB}$. This range overlaps with that computed numerically for the robust solution (i.e. $SE_{MC+VA} \in [5.7, 6.5] \text{ dB}$) showing the effectiveness of the model.

Furthermore, the simulations performed in order to find the robust solution can be exploited in order to obtain an analytical expression of the PF by means of the RSToolbox of Matlab®. This function can be employed to predict the PF and the corresponding range of variability even for not simulated parameter values.

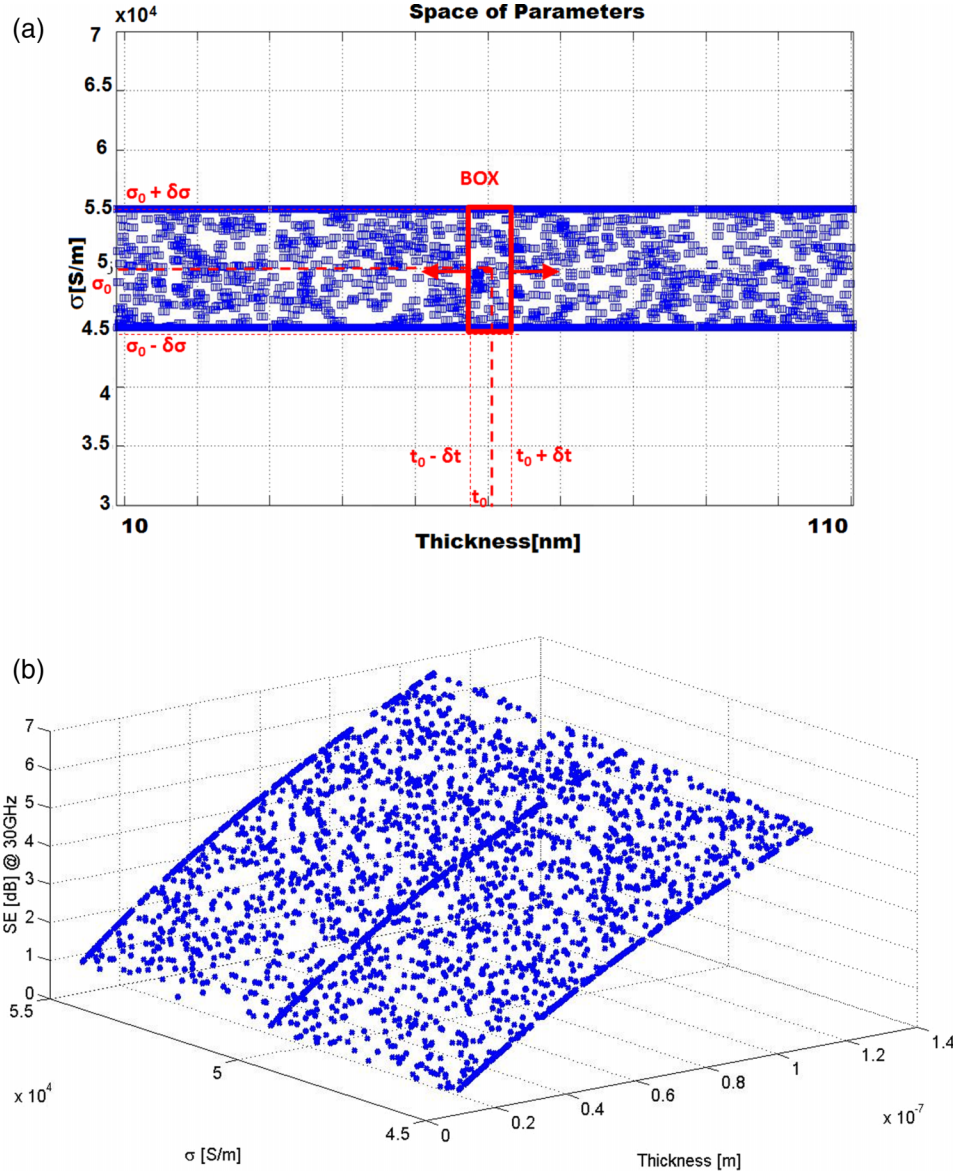


FIG. 4. a) Parameters space “thickness-conductivity of the PyC film” for the robust design of the shield with respect to δt and $\delta \sigma$ variation. The red box represents the “moving” region for the computation of the SE sensitivity. b) Solution space corresponding to the parameters space of Fig. 4(a): each point in the parameters space leads to a particular shield design characterized by the computed shielding effectiveness.

In particular, a second order polynomial can be adopted to represent in closed form the shielding effectiveness at $f=30\text{GHz}$ with respect to the “normalized” variables with confidence level of 1%:

$$SE(t, \sigma) = 3.865 + 2.696x_1 + 0.294x_2 + 0.179x_1x_2 - 0.418x_1^2 - 0.005x_2^2 \quad (5)$$

with $x_1 = [t - (t_{\max} + t_{\min})/2] / (t_{\max} - t_{\min})/2$ and $x_2 = [\sigma - (\sigma_{\max} + \sigma_{\min})/2] / (\sigma_{\max} - \sigma_{\min})/2$. The normalization in the interval $[-1, 1]$ is implemented to tackle the problems due to the different order of magnitude of the “actual” variables.³⁰

If the VA approach is considered on this function (i.e. by considering the function in (5) only on the vertices of the box), a direct bounding of the SE can be obtained which is indicated by the red

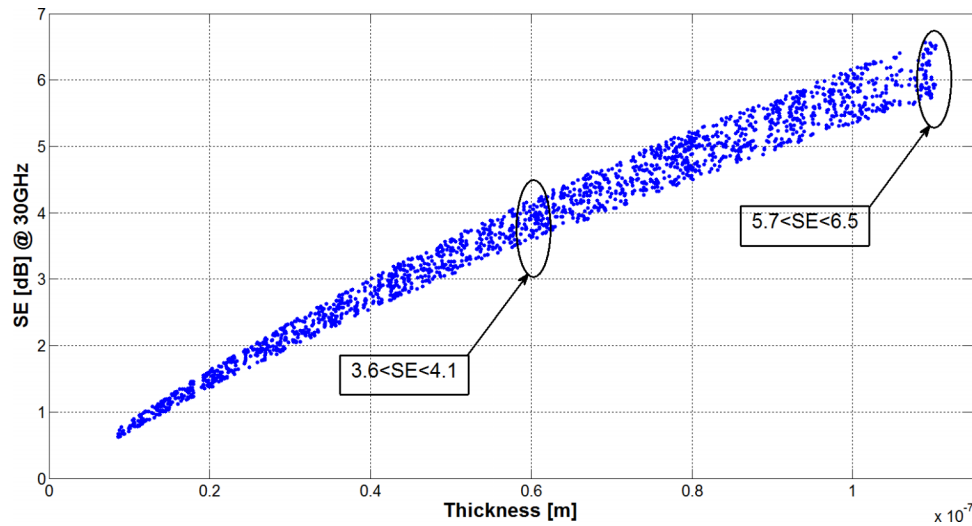


FIG. 5. Computed PF vs. the controllable parameter “thickness” in presence of variability on the uncontrollable parameter “conductivity”.

solid lines in Fig. 7 representing the minimum (lower-bound) and maximum (upper-bound) value of PF due to the supposed uncertainties.

In Fig. 7 also the MC estimations of the upper and lower bound are reported (blue lines). Such lines confirm that they are an underestimation of the actual PF bounding(Refs. 28 and 33) and justify the use of the VA to increase the reliability of the results in terms of robustness and worst case approach.

The analytical model, expressed by the second-order polynomial allows to predict the shielding effectiveness even when the thickness and the conductivity of the PyC are not simulated, but obtained experimentally.

As an example let us consider the data assumed in Ref. 8 where a nominal value of 25.2nm is reported for the PyC thickness. Its value is inside the parameter space for the controllable t factor, but with an uncertainty $\delta t=0.8$, higher than that adopted in the robust design searching algorithm. The reported sheet resistance in Ref. 8, R_t of 200 Ω /sq, leads to evaluate a nominal conductivity $\sigma_{\text{nom}}=(R_t \cdot t)^{-1} = 1.98 \times 10^5 \text{S/m}$ if as t value of 25.2nm is considered. By considering the uncertainty

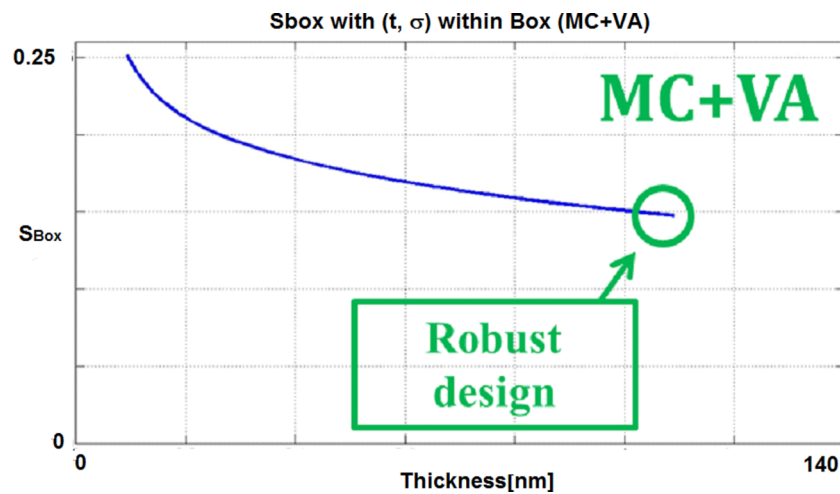


FIG. 6. Sensitivity index given in (4) as a function of the “controllable parameter” thickness. The minimum value furnishes the nominal solution leading to the robust design.

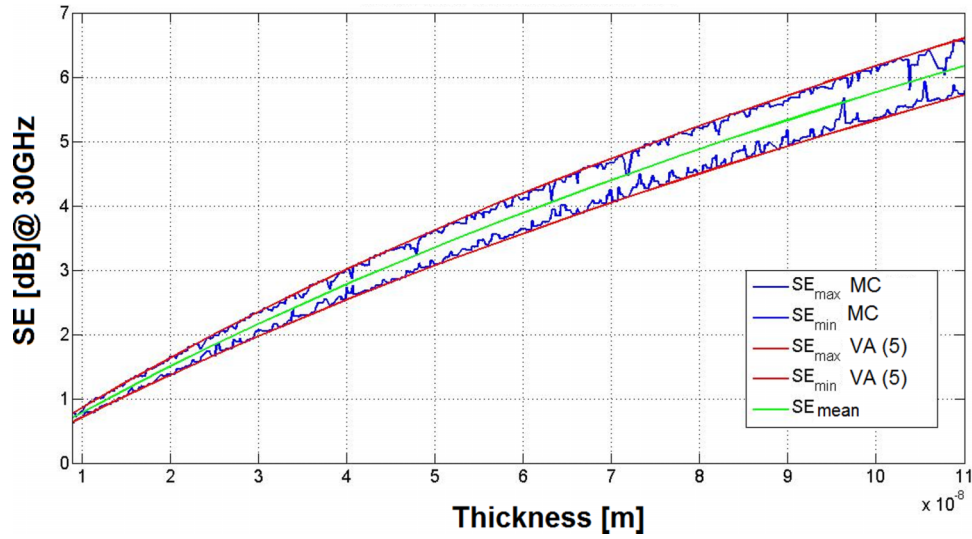


FIG. 7. Bounding of the SE obtained by applying VA on the analytical expression of the PF (red lines) compared with the MC computed (blue lines). In this figure also the mean value (green line) of the PF is reported.

due to the measurement technique, the reported δt variation leads to an effective PyC conductance in the range $[1.92, 2.05] \times 10^5 \text{ S/m}$ which in turn gives a $\delta\sigma$ equal to 3%. It means that the conductivity is out of the considered parameter space even if the narrower interval indicates that it is more accurate than that adopted in the robust design. Table II summarizes the parameter set of this particular design.

The normalized value of the PyC conductivity in Table II higher than 1 confirms that the set is out of the parameter space adopted in the previously considered simulation.

The experimental data of the 25-nm-thick PyC in Ka band in Ref. 8 leads to a shielding effectiveness of about 3.8 dB at a frequency of 30 GHz. Nevertheless, the basic measurement errors leads to $\delta|S_{21}| = \pm(0.6 + 0.06|S_{21}|) = \pm 0.83$ and therefore a measured SE, i.e. SE_{meas} , is in the range [2.97, 4.63] dB. The use of (5) with the nominal parameters reported in Table II leads to $SE_{\text{nom}} = 2.67 \text{ dB}$ that is very close to the left extreme of the experimentally detected one, despite the fact that combination of σ_0 e t_0 is out of the adopted parameters space of Fig. 4(a). It means that the considered polynomial interpolation is a good predictor for the SE at a given frequency. Moreover, if the parameters variations in Table II are taken in to account, the use of the VA on the equation (5) furnishes directly also the bounding of SE, $SE_{\text{RSM}} = [2.37, 2.95] \text{ dB}$, highlighting a deviation of about 10% with respect to the nominal value.

As far as the robust solution is considered, i.e. $(t, \sigma)_{\text{RD}} = (110 \text{ nm}, 5 \times 10^4 \text{ S/m})$, the use of (5) furnishes $SE_{\text{nom, RD}} = 6.14 \text{ dB}$ and a bounding $SE_{\text{RSM, RD}} = [5.66, 6.62] \text{ dB}$ as summarized in Table III.

The high reliability of the proposed design is confirmed by observing that only a 7% deviation from the nominal value of the shielding effectiveness is achieved in presence of 10% of variation on the PyC conductivity and an uncertainty of 0.3 nm on its thickness. This is true for both the $SE_{\text{MC+VA}}$, numerically computed from the data and for the SE_{RSM} , analytically evaluated by using (5). This leads to the conclusion that in order to keep reliable the SE it is advisable to

TABLE II. Nominal Value and corresponding variation of the design parameters external to the space considered for Fig. 4(a). Values according to the experimental data reported in Ref. 8.

Parameter name	PyC thickness	PyC conductivity
Nominal value	25.2 nm	$1.98 \times 10^5 \text{ S/m}$
Normalized nominal value	-0.679	29.700
Range variation	nominal $\pm 0.8 \text{ nm}$	nominal $\pm 3\%$

TABLE III. Robust design: parameters, assumed variation and range amplitude of the shielding effectiveness computed by the scattered data in Fig. 5 (SE_{MC+VA}) and according to (5) (SE_{RSM}).

Parameter name	PyC thickness	PyC conductivity	SE_{MC+VA}	SE_{RSM}
Nominal value	110 nm	50000 S/m	6.14 dB	6.14 dB
Range variation	nominal \pm 0.3nm	nominal \pm 10%	[5.7, 6.5]dB	[5.66, 6.62]dB

use thicker PyC layer. Obviously, the increasing thickness could correspond to a decrease in other performances of the system, as for example the transparency. However, multiobjective approach (that is out of the scope of this paper) can be considered in order to find the best compromise between reliability and transparency.

IV. CONCLUSION

A robust approach to the design of an electromagnetic shield based on a pyrolytic carbon layer thousands times thinner than skin depth is proposed. We demonstrated via a numerical approach, based on commercial software (COMSOL Multiphysics® and Matlab®) routines and a MC method, that even a deviation of 15-20% around the nominal values of the most important parameters for PyC film, i.e. its thickness and sheet resistance, would still lead to the desired level of EMI shielding effectiveness. Therefore, a reliable and robust design of the shielding performances can be achieved. Moreover, it can be observed that PyC layers, being scalable, chemically inert, significantly transparent in the visible range and with possibility to be deposited onto both metal or dielectric substrate, including flexible polymers, meet the high technological needs of graphene revolution and can be exploited from laboratory to mass production applications.

ACKNOWLEDGMENT

This work was supported by EU FP7 project FP7-604391 GRAPHENE Flagship and H2020-Adhoc-2014-20 project GA 696656 Graphene Core1; P.K. is thankful for the support by H2020 project CoEXaN and by Tomsk State University Competitiveness Improvement Program. Authors are thankful to Prof. Philippe Lambin (UNamur), Prof. Yuri Svirko (UEF) and Dr. Konstantin Batrakov (INP BSU) for their valuable comments and fruitful discussions.

- ¹ D.D.L. Chung, "Electromagnetic interference shielding effectiveness of carbon materials," *Carbon* **39**, 279-285 (2001).
- ² P. Kuzhir, A. Paddubskaya, D. Bychanok, A. Nemilentsau, M. Shuba, A. Plusch, S. Maksimenko, S. Bellucci, L. Coderoni, F. Micciulla, I. Sacco, G. Rinaldi, J. Macutkevici, D. Seliuta, G. Valusis, and J. Banys, "Microwave probing of nanocarbon based epoxy resin composite films: toward electromagnetic shielding," *Thin Sol. Film* **519**, 4114-4118 (2011).
- ³ V.K. Singh, A. Shukla, M.K. Patra, L. Saini, R.K. Jani, S.R. Vadera, and N. Kumar, "Microwave absorbing properties of a thermally reduced graphene oxide/nitrile butadiene rubber composite," *Carbon* **50**, 2202-2208 (2012).
- ⁴ P.P. Kuzhir, A.G. Paddubskaya, S.A. Maksimenko, V.L. Kuznetsov, S. Moseenkov, A.I. Romanenko, O.A. Shenderova, J. Macutkevici, G. Valusis, and Ph. Lambin, "Carbon onion composites for EMC applications," *IEEE Trans. Electromagn. Compat.* **54**, 6-16 (2012).
- ⁵ D. Bychanok, P. Kuzhir, S. Maksimenko, S. Bellucci, and C. Brosseau, "Characterizing epoxy composites filled with carbonaceous nanoparticles from dc to microwave," *J. App. Phys.* **113**, 124103.1 (2013).
- ⁶ P. Kuzhir, A. Paddubskaya, M. Shuba, S. Maksimenko, A. Celzard, V. Fierro, G. Amaral-Labat, A. Pizzi, J. Macutkevici, G. Valusis, J. Banys, S. Bistarelli, M. Mastrucci, F. Micciulla, I. Sacco, and S. Bellucci, "Electromagnetic shielding efficiency in Ka-band: carbon foam versus epoxy/CNT composites," *J. Nanophot.* **6**, 061715.1-18 (2012).
- ⁷ M. Letellier, J. Macutkevici, A. Paddubskaya, A. Plyushch, P. Kuzhir, M. Ivanov, J. Banys, A. Pizzi, V. Fierro, and A. Celzard, "Tannin-based carbon foams for electromagnetic applications," *IEEE EMC* **57**(5), 989-995, OCTOBER 2015, DOI: 10.1109/TEM.2015.2430370.
- ⁸ P. Kuzhir, A. Paddubskaya, S. Maksimenko, T. Kaplas, and Yu. Svirko, "Microwave Absorption Properties Of Pyrolytic Carbon Nanofilm," *Nanoscale Res. Lett.* **8**, Art No 60 (pp) (2013), doi:10.1186/1556-276X-8-60.
- ⁹ K. Batrakov, P. Kuzhir, S. Maksimenko, A. Paddubskaya, S. Voronovich, T. Kaplas, and Yu. Svirko, "Enhanced microwave shielding effectiveness of ultrathin pyrolytic carbon films," *Appl. Phys. Lett.* **103**, 073117 (2013); doi: 10.1063/1.48186802013.
- ¹⁰ M. Amin, M. Farhat, and H. Bağcı, "An ultra-broadband multilayered graphene absorber," *Opt Express* **21**(24), 29938-48, Dec 2 2013, doi: 10.1364/OE.21.029938.

- ¹¹ K. Batrakov, P. Kuzhir, S. Maksimenko, A. Paddubskaya, S. Voronovich, Ph Lambin, T. Kaplas, and Yu Svirko, "Flexible transparent graphene/polymer multilayers for efficient electromagnetic field absorption," *Sci. Rep.* **4**, Article number:7191 (2014), doi:10.1038/srep07191.
- ¹² F Qin and C Brosseau, "A review and analysis of microwave absorption in polymer composites filled with carbonaceous particles," *J. Appl. Phys.* **111**, 061301 (2012).
- ¹³ P. Kuzhir, A. Paddubskaya, A. Plyushch, N. Volynets, S. Maksimenko, J. Macutkevicius, I. Kranauskaitė, J. Banys, E. Ivanov, R. Kotsilkova, A. Celzard, V. Fierro, J. Zicans, T. Ivanova, R. Merijs Meri, I. Bochkov, A. Cataldo, F. Micciulla, S. Bellucci, and Ph. Lambin, "Epoxy composites filled with high surface area-carbon fillers: Optimization of electromagnetic shielding, electrical, mechanical, and thermal properties," *J. App. Phys.* **114**, 164304 (2013).
- ¹⁴ L. Guadagno, M. Raimondo, L. Vertuccio, M. Mauro, G. Guerra, K. Lafdi, B. De Vivo, P. Lamberti, G. Spinelli, and V. Tucci, "Optimization of graphene-based materials outperforming host epoxy matrices," *RSC Adv.* ISSN: 2046-2069 **5**, 36969-36978 (2015).
- ¹⁵ L. Guadagno, M. Raimondo, B. De Vivo, P. Lamberti, G. Spinelli, and V. Tucci, "Morphological and electrical characterization of epoxy resin filled with exfoliated graphite," in *proceeding of IEEE 15th International Conference on Nanotechnology (IEEE-NANO), 2015, Rome, 2015*, pp. 234-237, ISBN: 978-1-4673-8156-7, doi: 10.1109/NANO.2015.7388965.
- ¹⁶ R. Kotsilkova, E. Ivanov, I. Petrova, P. Kuzhir, D. Bychanok, K. Kouravelou, Th. Karachalios, A. Soto Beobide, G.A. Voyiatzis, D. Codegoni, F. Somaini, and L. Zanotti, "Nanoscale reinforcement of Polypropylene Composites with Carbon Nanotubes and Clay: Dispersion State, Electromagnetic and Nanomechanical Properties," *Polym. Eng. Sci.* (2016), about to be submitted to , DOI 10.1002/pen.24247 (2016).
- ¹⁷ B. De Vivo, P. Lamberti, R. Raimo, G. Spinelli, V. Tucci, L. Guadagno, M. Raimondo, L. Vertuccio, V. Vittoria, M. S. Sarto, and A. Tamburrano, "Electromagnetic and Mechanical Properties of a multiphase Carbon NanoTube/Clay/Epoxy Nanocomposite," in *proceedings of IEEE International Symposium on Electromagnetic Compatibility - EMC EUROPE Rome 17-21 september 2012* (Institute of Electrical and Electronics Engineers (IEEE)), pp. 1-6, ISBN: 9781467307161.
- ¹⁸ B. De Vivo, P. Lamberti, G. Spinelli, V. Tucci, L. Guadagno, M. Raimondo, L. Vertuccio, and V. Vittoria, "Improvement of the electrical conductivity in multiphase epoxy-based MWCNT nanocomposites by means of an optimized clay content," *Compos. Sci. Technol.* **89**, 69-76 (2013), ISSN: 0266-3538, DOI: 10.1016/j.compscitech.2013.09.021.
- ¹⁹ T Kaplas and Y Svirko, "Direct deposition of semitransparent conducting pyrolytic carbon films," *J. Nanophotonics* **6**, 061703 (2012).
- ²⁰ G. Dovbeshko, V. Romanyuk, D. Pidgirnyi, V. Cherepanov, E. Andreev, V. Levin, P. Kuzhir, T. Kaplas, and Yu. Svirko, "Optical properties of pyrolytic carbon films versus graphite and graphene," *Nanoscale Res. Lett.* **10**, 234 (2015), DOI 10.1186/s11671-015-0946-8.
- ²¹ T. Kaplas and P. Kuzhir, "Pyrocarbon reinforced graphene: synthesis and physical properties," *Nanoscale Res. Lett.* **11**, 54 (2016), doi:10.1186/s11671-016-1283-2.
- ²² A. Kaskela, A. G. Nasibulin, M. Y. Timmermans, B. Aitchison, A. Papadimitratos, Y. Tian, Z. Zhu, H. Jiang, D. P. Brown, A. Zakhidov, and E. I. Kauppinen, "AerosolSynthesized SWCNT Networks with Tunable Conductivity and Transparency by a Dry Transfer Technique," *Nano Lett.* **10**(11), 4349-4355, Nov. 2010.
- ²³ R. X. K. Gao, W. J. R. Hoefer, T. S. Low, and E. P. Li, "Robust design of electromagnetic wave absorber using the taguchi method," *IEEE Trans. Electromagn. Compat.* **55**, 1076-1083 (2013).
- ²⁴ M. Lobet, N. Reckinger, L. Henrard, and P. Dans Lambin, "Robust electromagnetic absorption by graphene/polymer heterostructures," *Nanotechnology* **26**(28), 9, 285702, DOI 10.1088/0957-4484/26/28/285702.
- ²⁵ Y. Wu and A. Wu, *Taguchi Methods for Robust Design* (ASME Press, 2000).
- ²⁶ R. Spence and R. S. Sooin, *Tolerance design of electronic circuits* (Imperial College Press, 1988).
- ²⁷ P. Lamberti, "Progetto robusto di circuiti con parametri incerti," Ph.D. Thesis, University of Salerno, ITALY, 2005.
- ²⁸ P. Lamberti, M. S. Sarto, V. Tucci, and A. Tamburrano, "Robust design of high-speed interconnects based on an MWCNT," *IEEE Trans. Nanotechnol.* **11**(4), 799-807. art. no. 6198897 (2012), doi: 10.1109/TNANO.2012.2198922.
- ²⁹ D. C. Montgomery, *Design and Analysis of Experiments*, 5th ed. (John Wiley & Sons, 2001).
- ³⁰ R. H. Myers and D. C. Montgomery, *Response Surface Methodology – Process and Product Optimization Using Designed Experiments*, 2nd ed. (John Wiley & Sons, 2002).
- ³¹ Richard B. Schulz and V. C. Plantz, "Shielding theory and Practice," *IEEE Trans. Electromagn. Compat.* **30**(3), August 1988.
- ³² E. Giusti, in *Analisi matematica I*, edited by B. Boringhieri (1993).
- ³³ P. Lamberti and V. Tucci, "Impact of the Variability of the Process Parameters on CNT-based Nanointerconnects Performances: a Comparison Between SWCNTs Bundles and MWCNT," *IEEE Trans. Nanotechnol.* **11**, 924-933 (2012), ISSN: 1536-125X.